GENERALISED ELEMENT LOAD METHOD WITH WHOLE DOMAIN ACCURACY FOR RELIABLE STRUCTURAL DESIGN

Chi-Kin Iu

Lecturer, *School of Civil Engineering and Built Environment*
Queensland University of Technology
QUT Brisbane, QLD, Australia
(Corresponding author: E-mail: iu.jerryu@gmail.com)

Received: 6 November 2015; Revised: 29 November 2015; Accepted: 7 December 2015

ABSTRACT: This paper presents a formulation to capture all kinds of second-order effects (i.e. discrete nodal displacement as the numerical approach: P-δ & P-Δ effect, large displacement, snap-through buckling, initial imperfection, etc.) for members under loads along their lengths. The efficient computational formulation of the generalised element load method (GELM) is proposed which gives accurate element and nodal solutions when using the one-element-per-member model. It is believed the GELM provides a reliable and efficient method for improving the second-order analysis for design of practical structures.

Keywords: Generalised element load method; second-order elastic analysis; one element per member; higher-order element formulation; initial imperfection; element solutions

DOI:10.18057/IJASC.2016.12.4.6

1. INTRODUCTION

Nonlinear numerical analysis for a structure was prevalent from the past half century, likely because of availability of low-cost and powerful computers. The popular displacement-based finite element approach was devoted by (hierarchic displacement element: mesh refinement required) a number of scholars; Meek and Tan [1], Chan and Kitipornchai [2] and Iu and Bradford [3][4] among others and hence the conventional displacement-based finite element approach have been well established.

In spite of its robustness, versatility and applicability, the conventional displacement-based finite element analysis possesses a drawback of element discretisation for a member to give accurate solutions when loads are along a member. To overcome the drawback, Chan and Zhou [5][6] presented a PEP finite element to simulate the second-order effect on a member with an initial geometric imperfection. Izzuddin [7] later formulated a fourth-order displacement-based finite element for structures under thermal loads. Iu and Bradford [8] provided a higher-order finite element analysis to examine various kinds of geometric nonlinearities for framed structures using a single element per member.

Previous methods and their applications on second-order analysis for members under element loads are very limited to conversion of element loads to the nodal solutions and hence the major setback of these approaches is less accurate solutions obtained when using a single element to simulate a member with loads along its length. In order to take the element load effect into account for the member behaviour, Zhou and Chan [9, 10] presented a second-order elastic analysis that is capable of modelling the element load effect in the element stiffness formulation, in lieu of by a system analysis for the nodal solutions. Unfortunately, each element load case requires a specific element stiffness matrix, which is limited in practical applications because of the multiplicity of load patterns imposed on an element. And also no accurate solution along an element was evaluated in their research works.

Research in forced-based finite element approach seems to lag behind its displacement-based counterpart. To overcome the obstacle of the flexibility approach, Neuenhofer and Filippou [11] developed a procedure for determining the nonlinear element state. Later, Neuenhofer and Filippou [12] extended their work to study the effects of force distribution along a single element and it is another element force solution. Their flexibility approach (i.e. Valipour and Bradford [13]), in principle, is difficult to evaluate the deformation accurately along a single element when compared to the displacement-based stiffness approach.

In summary, the objective of research on higher-order element by the one-element-per-member approach is confined to the use of less elements for a structure with accurate nodal solutions of its members under element loads. As a result, the accurate element solutions cannot be obtained when an element is subjected to element load. It means that a reliable structural analysis for members subjected to external element loads is unavailable with an error contained in analysis by one-element-per-member model for members with loads along the lengths. The lumping and consistent load methods alone are unable to produce accurate first- and second-order elastic solutions due to element load effect within an element itself as reported by Iu and Bradford [14] and Iu [15]. In this paper, a qualified element for these purposes is proposed and it transforms the traditional discretised nodal solution into continuous displacement and force element solutions for the geometric nonlinear effects. As a natural result, the present method can ensure the adequate and reliable structural safety for the whole domain not only at the element nodes, but also along an element, when one-element-per-member model is adopted. This method strikes a balance between simplicity in the formulation (similar stiffness form preserved) and accuracy in describing the element load effect for both nodal (robust system analysis) and element responses (sophisticated element formulation).

2. STIFFNESS FORMULATION FOR HIGHER-ORDER ELEMENT WITH ELEMENT LOAD EFFECTS

The internal strain energy U due to axial strain ε_x and twist strain γ_x in the continuum medium are considered to formulate the stiffness matrices of the present higher-order beam-column element. Axial strain ε_x is expressed through linear axial deformation and the nonlinear elastic transverse displacement function [Iu [15]] of which the strain energy dissipated in flexural bending and member bowing are consisted. The internal strain energy U caused by the axial strain ε_x and twist strain γ_x along the beam-column continuum can be accumulated by integration of $\delta U_A = E\varepsilon_x \delta\varepsilon_x$ and of $\delta U_T = G\gamma_x \delta\gamma_x$ over the domain of element length and element section, which can be expressed in terms of u, v, w and ϕ from an appropriate expansion of Green's strain tensor as

$$U = \int_{Vol}\left(\int_{\varepsilon_x} E\varepsilon_x \,\mathrm{d}\,\varepsilon_x + \int_{\gamma_x} G\gamma_x \,\mathrm{d}\,\gamma_x\right)\mathrm{d}Vol = \tfrac{1}{2}\int_{Vol}\left(E\varepsilon_x^2 + G\gamma_x^2\right)\mathrm{d}Vol\,, \tag{1}$$

The internal strain energy U including various components becomes

$$U = \int \delta U = E\int_{Vol}\int_{\varepsilon_x} \varepsilon d\varepsilon dV = \frac{E}{2}\int_{Vol}\varepsilon_x^2 dVol$$

$$\begin{aligned} U = {} & \frac{EA}{2}\int_L\left(\frac{\mathrm{d}u}{\mathrm{d}x}\right)^2\mathrm{d}x + \frac{P}{2}\int_L\left(\frac{\mathrm{d}v}{\mathrm{d}x}\right)^2\mathrm{d}x + \frac{P}{2}\int_L\left(\frac{\mathrm{d}w}{\mathrm{d}x}\right)^2\mathrm{d}x + \frac{EI_z}{2}\int_L\left(\frac{\mathrm{d}^2v}{\mathrm{d}x^2}\right)^2\mathrm{d}x \\ & + \frac{EI_y}{2}\int_L\left(\frac{\mathrm{d}^2w}{\mathrm{d}x^2}\right)^2\mathrm{d}x + \frac{GJ}{2}\int_L\left(\frac{\mathrm{d}\phi}{\mathrm{d}x}\right)^2\mathrm{d}x \end{aligned} \tag{2}$$

in which u, v and w are dependent variables for axial deformation, for lateral deflections in the direction in y-axis and z-axis, respectively, which is given in [Iu [15]]; ϕ is for twist angle about x-axis; EA, EI and GJ are the axial rigidity, flexural rigidity about corresponding axes and torsional rigidity, respectively; P is the axial element load.

In this study, external loads produce by nodal load $\mathbf{f}_k$ and element load $\mathbf{\Phi}_k$. Hence, the external work done V constitutes two components; first component V_f (Lumping load method) is the work done by nodal loads $\mathbf{f}_k$ in going through nodal displacements $\mathbf{u}_k$; second component V_Φ (Consistent load method) is the work done by transverse element load $\mathbf{\Phi}_k$ in going through the assumed transverse displacement field associated with the element displacement function $\mathbf{N}$ over the element length. In accord with the assumption of conservative loads, the work done going through the deflected element $\mathbf{N}$ due to element loads is independent of the axial load q at all stages, such as setting $q = 0$ in the higher-order element function in [Iu [15]][15], as given by

$$V = V_\Phi + V_f = \int_L \mathbf{u}_k^{\mathrm{T}} \mathbf{N}^{\mathrm{T}} \mathbf{\Phi}_k dx + \mathbf{u}_k^{\mathrm{T}} \mathbf{f}_k . \tag{3}$$

The elastic force-displacement relationship is derived from the total potential energy of the general beam-column element subjected to both nodal and element loads. The total potential energy for nonlinear elastic analysis of column-beam element is the summation of internal strain energy U in Eq. 2 and external work done V in Eq. 3 as

$$\begin{aligned} \Pi = {} & \frac{EA}{2}\int_L \left(\frac{\mathrm{d}u}{\mathrm{d}x}\right)^2 \mathrm{d}x + \frac{P}{2}\int_L \left(\frac{\mathrm{d}v}{\mathrm{d}x}\right)^2 \mathrm{d}x + \frac{P}{2}\int_L \left(\frac{\mathrm{d}w}{\mathrm{d}x}\right)^2 \mathrm{d}x + \frac{EI_z}{2}\int_L \left(\frac{\mathrm{d}^2 v}{\mathrm{d}x^2}\right)^2 \mathrm{d}x \\ & + \frac{EI_y}{2}\int_L \left(\frac{\mathrm{d}^2 w}{\mathrm{d}x^2}\right)^2 \mathrm{d}x + \frac{GJ}{2}\int_L \left(\frac{\mathrm{d}\phi}{\mathrm{d}x}\right)^2 \mathrm{d}x - \int_L \mathbf{u}_k^{\mathrm{T}} \mathbf{N}^{\mathrm{T}} \mathbf{\Phi}_k dx - \mathbf{u}_k^{\mathrm{T}} \mathbf{f}_k \end{aligned} \tag{4}$$

where $\mathbf{u}_k$ and $\mathbf{f}_k$ are the column vectors of the displacement and external applied force with respect to the corresponding degrees of freedom, respectively. $\mathbf{u}_k$ is a column vector as given by $\left\langle \Delta u, \theta_{z1}, \theta_{z2}, \Delta\theta_x, \theta_{y1}, \theta_{y2} \right\rangle^T$ in notations, in which $\Delta u = u_1 - u_2$ and $\Delta\theta_x = \phi_1 - \phi_2$.

The equilibrium equation of higher-order element subjected to the general transverse element load can be obtained by first variation of total potential energy functional of Eq. 4 for a stable structure as,

$$\delta\Pi = \frac{\partial}{\partial \mathbf{u}_k}(U - V)\delta\mathbf{u}_k = 0 \tag{5}$$

for which the internal strain energy of Eq. 2 depends not only on the dependent variables $\mathbf{u}_k$, but also on the axial load parameter q, and thereby the differential operator becomes

$$\frac{\partial}{\partial \mathbf{u}_k} = \frac{\partial}{\partial \mathbf{u}_k} + \frac{\partial q}{\partial \mathbf{u}_k} \cdot \frac{\partial}{\partial q} . \tag{6}$$

According to the Eq. 5, the nonlinear equilibrium equation is provoked as,

$$\begin{aligned}\delta\Pi &= \left(\frac{\partial U}{\partial \mathbf{u}_k}+\frac{\partial U}{\partial q}\cdot\frac{\partial q}{\partial \mathbf{u}_k}-\frac{\partial V_\Phi}{\partial \mathbf{u}_k}-\frac{\partial V_\Phi}{\partial q}\cdot\frac{\partial q}{\partial \mathbf{u}_k}-\frac{\partial V_f}{\partial \mathbf{u}_k}\right)\delta\mathbf{u}_k = 0\\ &= \left(\frac{\partial U}{\partial \mathbf{u}_k}+\frac{\partial U}{\partial q}\cdot\frac{\partial q}{\partial \mathbf{u}_k}-\frac{\partial V_\Phi}{\partial \mathbf{u}_k}-\mathbf{f}_k\right)\delta\mathbf{u}_k = 0\end{aligned} \tag{7}$$

in which it is noteworthy that the terms of $\partial V_\Phi/\partial q\cdot\partial q/\partial \mathbf{u}_k$ in Eq. 7 can be neglected. If the local nonlinear effect of axial load q in V_Φ is taken into account ($\partial V_\Phi/\partial q\cdot\partial q/\partial \mathbf{u}_k \neq 0$), the reliable convergent of this nonlinear analysis cannot be preserved, while the total external load level of a structure depends on the element deformations, which violates against the assumption of conservative load of this study. The element resistance or the secant stiffness formulation can be obtained from

$$\begin{aligned}M_{\alpha 1} = \frac{\partial U}{\partial \theta_{\alpha 1}} &= \frac{EI_\alpha}{L}\left[\frac{19200+800q+\frac{61}{7}q^2+\frac{23}{1260}q^3}{(80+q)^2}+\frac{2304+288q+\frac{29}{5}q^2+\frac{11}{420}q^3}{(48+q)^2}\right]\theta_{\alpha 1}\\ &+\frac{EI_\alpha}{L}\left[\frac{19200+800q+\frac{61}{7}q^2+\frac{23}{1260}q^3}{(80+q)^2}-\frac{2304+288q+\frac{29}{5}q^2+\frac{11}{420}q^3}{(48+q)^2}\right]\theta_{\alpha 2}\\ &+\frac{EI_\alpha}{L}\left[-\frac{q^2\overline{M}_0}{210(48+q)^2}-\frac{q^2\overline{S}_0 L}{630(80+q)^2}\right]\end{aligned} \tag{8}$$

$$\text{or}\quad M_{\alpha 1} = \frac{EI_\alpha}{L}\left(C_1\,\theta_{\alpha 1}+C_2\,\theta_{\alpha 2}-C_m\overline{M}_0-C_s\overline{S}_0 L\right), \tag{9}$$

$$\begin{aligned}M_{\alpha 2} = \frac{\partial U}{\partial \theta_{\alpha 2}} &= \frac{EI_\alpha}{L}\left[\frac{19200+800q+\frac{61}{7}q^2+\frac{23}{1260}q^3}{(80+q)^2}+\frac{2304+288q+\frac{29}{5}q^2+\frac{11}{420}q^3}{(48+q)^2}\right]\theta_{\alpha 2}\\ &+\frac{EI_\alpha}{L}\left[\frac{19200+800q+\frac{61}{7}q^2+\frac{23}{1260}q^3}{(80+q)^2}-\frac{2304+288q+\frac{29}{5}q^2+\frac{11}{420}q^3}{(48+q)^2}\right]\theta_{\alpha 1}\\ &+\frac{EI_\alpha}{L}\left[\frac{q^2\overline{M}_0}{210(48+q)^2}-\frac{q^2\overline{S}_0 L}{630(80+q)^2}\right]\end{aligned} \tag{10}$$

$$\text{or}\quad M_{\alpha 2} = \frac{EI_\alpha}{L}\left(C_1\,\theta_{\alpha 2}+C_2\,\theta_{\alpha 1}+C_m\overline{M}_0-C_s\overline{S}_0 L\right) \tag{11}$$

in which the subscript α denotes y or z, and

$$\begin{aligned}P = P_1 - P_2 &= \frac{\partial U}{\partial e}+\frac{\partial U}{\partial q}\cdot\frac{\partial q}{\partial e}\\ &= \frac{EAe}{L}+EA\sum_{\alpha=y,z}\Big[b_1(\theta_{\alpha 1}+\theta_{\alpha 2})^2+b_2(\theta_{\alpha 1}-\theta_{\alpha 2})^2\\ &\qquad +b_{m1}(\theta_{\alpha 1}-\theta_{\alpha 2})\overline{M}_0+b_{s1}(\theta_{\alpha 1}+\theta_{\alpha 2})\overline{S}_0 L+b_{m2}\overline{M}_0^2+b_{s2}\overline{S}_0^2 L^2\Big]\\ &= EA\left[\frac{e}{L}+\sum_{\alpha=y,z}\left(C_b+b_{m1}(\theta_{\alpha 1}-\theta_{\alpha 2})\overline{M}_0+b_{s1}(\theta_{\alpha 1}+\theta_{\alpha 2})\overline{S}_0 L+b_{m2}\overline{M}_0^2+b_{s2}\overline{S}_0^2 L^2\right)\right]\end{aligned} \tag{12}$$

in which

$$b_1 = \frac{12800 + 2080q/7 + 46q^2/21 + 23q^3/2520}{(80+q)^3}; \tag{13}$$

$$b_2 = \frac{4608 + 672q/5 + 66q^2/35 + 11q^3/840}{(48+q)^3}; \tag{14}$$

$$b_{m1} = \frac{-16q}{35(48+q)^3}; \tag{15}$$

$$b_{m2} = \frac{12/35 + q/105}{(48+q)^3}; \tag{16}$$

$$b_{s1} = \frac{-16q}{63(80+q)^3}; \tag{17}$$

$$b_{s2} = \frac{20/63 + q/315}{(80+q)^3}. \tag{18}$$

Right subscript symbol *m* and *s* in Eqs. (13) to (18) stand for the contribution from moment $\overline{M}_0$ and shear force $\overline{S}_0$ component, respectively. C_m and C_s provoke the second-order moment due to coupling effect of both axial and lateral element loads, whereas b_{m1}, b_{m2}, b_{s1} and b_{s2} exhibit axial force resistance subjected to the coupling effect. However, when axial load q does not exist, b_{m1} and b_{s1} vanish and hence the coupling effect between the axial force and the lateral loads is eliminated. On the contrary, i.e. $q=0$, b_{m2} and b_{s2} still take part in providing the axial tensile resistance P in Eq. 12 that means element load exerting the positive axial resistance P due to elongation. It can be seen that the secant stiffness coefficients, such as C_m, C_s, b_{m1}, b_{m2}, b_{s1} and b_{s2} accounting for the element load effect in Eqs. 9, 11, 13 to 18 varying from different load cases by adjusting $\overline{M}_0$ and $\overline{S}_0$, can contribute to the nodal solutions insignificantly. It means the element load effect on the nodal solutions is well replicated by the lumping and consistent load method except the buckling modes, at which the common denominators ($48+q$) and ($80+q$) vanish in order to magnify the nodal solutions from Eqs. 8 to 12, corresponding to symmetric and anti-symmetric buckling modes, respectively.

Because of load-dependent characteristic in the internal strain energy, the coupling effect between external element load and deformations becomes inherent in the present stiffness formulation from Eq. 8 to 12. The Eq. 12 contains two independent bowing functions, which are symmetric and complete, while both force equilibrium equations of bending moment and shear force are incorporated into this element stiffness formulation. Instead of the lumping load and consistent load method formulated through the work done, the generalised element load method (GELM) can measure the strain energy dissipated into an element due to element load coupling with axial load effect that disregard in member bowing and flexural terms of the strain energy equation as Eq. 4. It means it regards the different strain energy terms as individual independent component. Because of this, the element load terms, such as $\overline{M}_0$ and $\overline{S}_0$, vanish or become very insignificant when subjected to no axial load. The element load method heralds the element load can cause the additional internal strain energy dissipation into both member bowing and flexural components as nodal solutions when subjected to axial compression.

It is of importance to note that, despite subjected to different element loads, the line integration in Eq. 4 is identically carried out along the domain of an element, as the pattern of displacement function in [Iu [15]] remains unchanged regardless of a variety of element loading distribution but the magnitude of element load coefficients $\overline{M}_0$ and $\overline{S}_0$. It produces a crucial insight that the principle of superposition is valid to integrate the individual element load type $\overline{M}_0$ and $\overline{S}_0$ as listed in Appendix I in order to form a general element load case respectively in advent of nonlinear analysis being implemented, and subsequently can be allowed for by updating the element load coefficients $\Delta\lambda \cdot \overline{M}_0$ and $\Delta\lambda \cdot \overline{S}_0$ in the course of the system solution procedures as mentioned in Section 3. Therefore, the second-order solution due to a diverse kind of element loading can be unified by summing up the standardized and fundamental simple element load cases given in Appendix I of [Iu [15]]. This unique feature avoids tedious and enormous stiffness coefficients under a considerable combination of general element loads, and hence leads to a versatile stiffness formulation in the form of simplicity and brevity.

The tangent stiffness matrix can be obtained by taking a second differentiation of the total potential energy functional in Eq. 4 with respect to the dependent variables $\mathbf{u}_k$ and axial load q. When the external work done V is linear as aforementioned, the tangent stiffness can be derived by second derivative of internal strain energy U as given by

$$\mathbf{K}_t = \frac{\partial^2 \Pi}{\partial \mathbf{u}_j \partial \mathbf{u}_k} = \frac{\partial}{\partial \mathbf{u}_j}\left(\frac{\partial U}{\partial \mathbf{u}_k}\right) + \frac{\partial}{\partial \mathbf{u}_k}\left(\frac{\partial U}{\partial q} \cdot \frac{\partial q}{\partial \mathbf{u}_j}\right). \tag{19}$$

The tangent stiffness of the present beam-column element with element load effect can then be written in Eq. 20, which relates the incremental deformation to the corresponding external loads imposed on an element in the member coordinate.

$$\mathbf{K}_t = \frac{EI}{L}\begin{bmatrix} \frac{1}{L^2 H} & \frac{G_{y1}}{LH} & \frac{G_{z1}}{LH} & 0 & \frac{G_{y2}}{LH} & \frac{G_{z2}}{LH} \\ & \xi_y\left(C_1 + \frac{G_{y1}^2}{H}\right) & \frac{G_{y1}G_{z1}}{H} & 0 & \xi_y\left(C_2 + \frac{G_{y1}G_{y2}}{H}\right) & \frac{G_{y1}G_{z2}}{H} \\ & & \xi_z\left(C_1 + \frac{G_{z1}^2}{H}\right) & 0 & \frac{G_{z1}G_{y2}}{H} & \xi_z\left(C_2 + \frac{G_{z1}G_{z2}}{H}\right) \\ & & & \eta & 0 & 0 \\ & \textit{symmetric} & & & \xi_y\left(C_1 + \frac{G_{y2}^2}{H}\right) & \frac{G_{y2}G_{z2}}{H} \\ & & & & & \xi_z\left(C_1 + \frac{G_{z2}^2}{H}\right) \end{bmatrix} \tag{20}$$

in which the coefficients G_n and H expressed in the tangent stiffness formulation in Eq. 20 are shown in the Appendix I. I is the second moment of inertia about the axis in which the buckling effect is considered. Also $\xi_z = I_z/I$ and $\xi_y = I_y/I$. The tangent stiffness matrix should assemble and transform into global coordinate as written in Eq. 21, as the incremental nodal displacements of a structure can then be obtained by tangent stiffness relationship.

$$\mathbf{K}_T = \sum_{\text{elements}} \mathbf{L}\,\mathbf{K}_e\,\mathbf{L}^{\mathrm{T}} = \sum_{\text{elements}} \mathbf{L}\left(\mathbf{T}^{\mathrm{T}}\,\mathbf{K}_t\,\mathbf{T} + \mathbf{N}\right)\mathbf{L}^{\mathrm{T}}, \tag{21}$$

in which **T** is transformation matrix relating the member forces to element force in local coordinate. **L** is the transformation matrix from local ordinate to global coordinate. And **N** is a stability matrix to allow for the work done of rigid body motion.

3. SYSTEM SOLUTION PROCEDURES

For being well-formulated to yield the accurate solutions, the fundamental physical laws must incorporate to govern behaviour of a structure properly; they are force equilibrium equation, compatibility condition and material law, which can be accounted for at the system level when resorted to the numerical method (nodal solution). To evaluate the nonlinear elastic behaviour of a structure, the equilibrium solution at the nodes within $\Delta\lambda$ load factor can be given as,

$$\Delta\mathbf{f}^n = \mathbf{f}^n - \mathbf{R}_i^n = \mathbf{K}_T \Delta\mathbf{u}_i^n, \tag{22}$$

with which the law of compatibility condition of a structural system is complied. And the elastic material law is embodied in the stiffness formulation, i.e. $\mathbf{K}_T$. Therefore, the total nodal deformations can be written as,

$$\Delta\mathbf{u}_i^n = \mathbf{K}_T^{-1}\Delta\mathbf{f}^n; \quad \mathbf{u}_{i+1}^n = \mathbf{u}_i^n + \Delta\mathbf{u}_i^n \tag{23);(24}$$

The nodal element resistance can be evaluated either dependent of total deformations $\mathbf{u}_{i+1}^n$ as written,

$$\overline{\mathbf{u}}_{i+1}^n = \mathbf{L}^T\mathbf{u}_{i+1}^n; \overline{\mathbf{R}}_{i+1}^n = \mathbf{K}_s\overline{\mathbf{u}}_{i+1}^n; \mathbf{R}_{i+1}^n = \mathbf{L}\overline{\mathbf{R}}_{i+1}^n \tag{25);(26);(27}$$

in which $\overline{\mathbf{u}}_i^n$ and $\overline{\mathbf{R}}_i^n$ are respectively total deformations and nodal element resistance at element level. The unbalanced force at *n*-th load increment is therefore obtained as,

$$\Delta\mathbf{f}^n = \mathbf{f}^n - \mathbf{R}_{i+1}^n \tag{28}$$

The above process is repeated until the unbalanced forces $\Delta\mathbf{f}^n$ at the nodes are eliminated, and the next $(n+1)$-th load increment $\mathbf{f}^{n+1}$ as given in Eq. 29 should begin until numerical instability.

$$\mathbf{f}^{n+1} = \mathbf{f}^n + \Delta\lambda\mathbf{f} \tag{29}$$

By satisfying these three conditions at global system level, the solutions of deformations $\mathbf{u}_{i+1}$ and element resistances $\mathbf{R}_{i+1}$ at equilibrium point can be attained at the nodes of the elements at global system level only, and no accurate element solutions at element level can be secured according to the above system solution procedures. Therefore, the system solution procedures alone do not suffice to yield the accurate element solutions. On contrary, the present higher-order element, which satisfies all three conditions of physical law at element level, enables to replicate the accurate first- and second-order elastic element solutions.

For the sake of applicability, the principle of superposition is favourably applied. To this end, the element loading distribution is converted into a single loading magnitude (i.e. $\overline{M}_0$ & $\overline{S}_0$) at mid-span in order to provide the initial perturbation for triggering the second-order member bowing effect due to its transverse element loads. In other words, this approach is a trade-off between the distribution of element load effect and the generality of a plethora of element stiffness under a diverse kind of element load cases. Meanwhile, the magnitude of both equivalent moment $\overline{M}_0$ and shear $\overline{S}_0$ components are updated to corresponding load level as Eq. 29 according to load factor $\Delta\lambda$ to measure the second-order member bowing effect commensurate at each specific load level.

4. VERIFICATION EXAMPLES

The objective of this paper is on the accurate element solutions together with the nodal behaviour, which are compared with the nodal solution from the others. Hence, the ranges of the validity of the proposed numerical analysis are on the second-order elastic displacements and forces including the large deformation, P-δ & P-Δ effect, snap-through buckling behaviour, are numerically exemplified through several examples, which were reported by independent studies. Finally, the side-track application by using this GELM is the initial imperfection as shown in this Section.

4.1 Second-order Member Bowing effect (P-δ effect)

4.1.1 Superposition principle valid in second-order member bowing effect

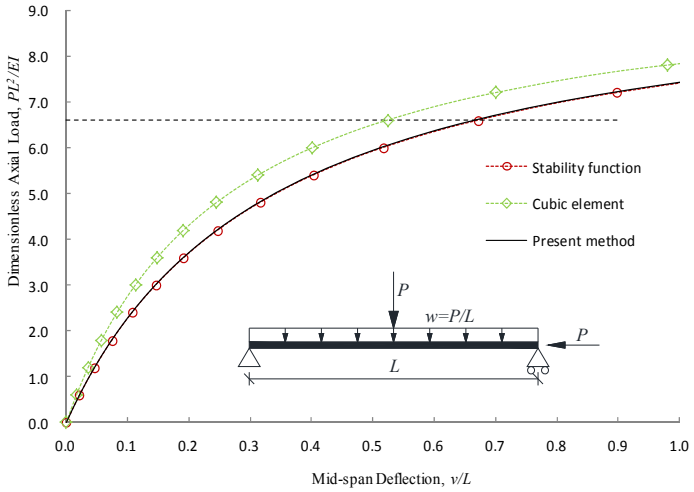

Figure 1. Second-order Bowing Effect of a Simple Supported Element under Element Combined Load

The present example exemplifies second-order member bowing effect on a simple supported element subjected to combination loads of uniform distributed load and point load. And, eventually, it leads to profound implication of using superposition principle for load combination, which can facilitate its application without loss of accuracy. The nonlinear solution procedure of incorporating element load effect in the second-order behaviour using superposition principle is studied.

Figure 1 indicates the mid-span deflection of an element using different approaches subjected to the load combination and axial compression. Similarly, present method can well capture the first-order bending due to element load and second-order coupling effect between element load and axial compression. Further, the element displacement and force solutions at highly second-order regime, which is illustrated in Figure 1 by horizontal dashed line, are well represented by the present method as shown in Figures 2 & 3, respectively.

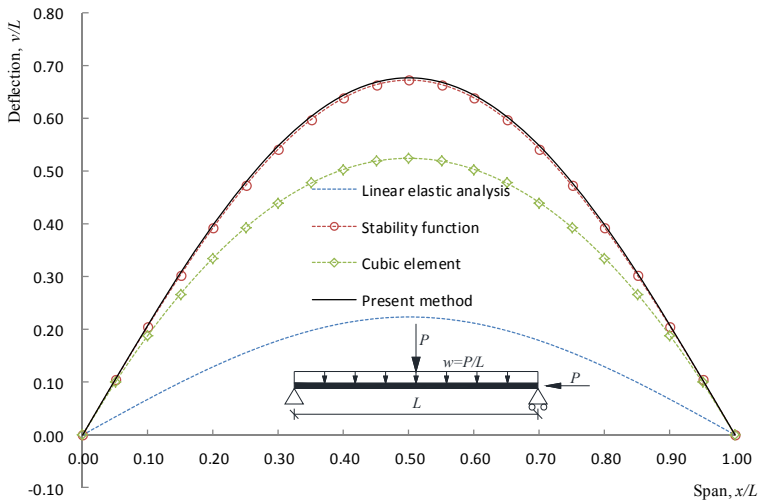

Figure 2. Deflections Along a Simple Supported Element under Combined Load Subjected to P-δ Effect

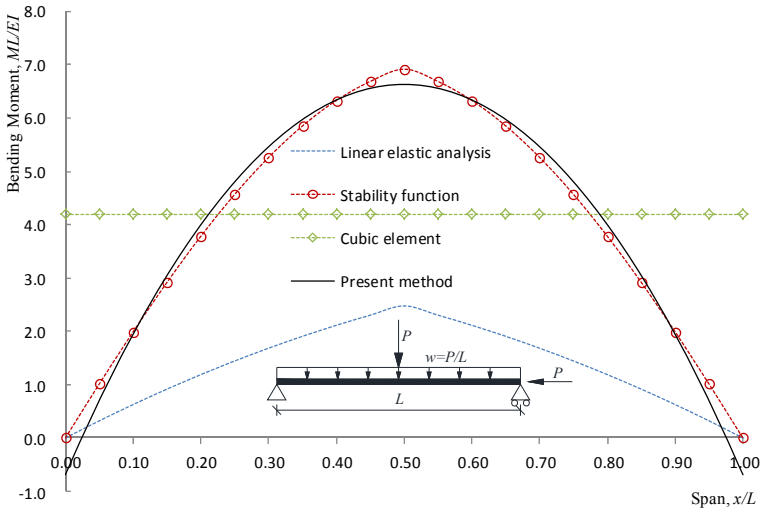

Figure 3. Bending Moment Along a Simple Supported Element under Combined Load Subjected to P-δ Effect

In conclusion, the present method can achieve the high level of accuracy in element deflection at all ranges particularly. Moreover, the profound insight of this example is that the superposition principle is valid to evaluate the second-order coupling P-δ effect due to the element loads. The present higher-order element function can therefore generalize and replace the multiplicity of the stability functions with particular element load cases. In addition, the present higher-order continuous function can reproduce the various kinds of element solution subjected to various element loads, even the discontinuous point load and their combination load case. It is noteworthy that there is a trivial bending moment at pinned end. This inaccuracy is attributed to that no force equilibrium condition is enforced at the element nodes at element level. Under this circumstance, the nodal force solution can be adopted at the supports instead.

4.2 Large Deformation Behaviour

4.2.1 Large deformation of a simply supported element under uniform load

This example aims at validating the capacity of the present element load method to capture the large deformation of a structure, including the deformations and load distribution along an element. A simple supported beam under uniform load is studied as shown in Figure 4, whose mid-span deflection and end nodal axial displacement are also plotted against the load factor λ. And the load level P is 10kN and the dimensions and sections of the element are normalized as the previous examples. In this example, the present method is compared with others, including NIDA [16] and Iu and Bradford . The axial deformation and mid-span deflection among all three methods are very consistent as shown in Figure 4, at which the axial deformation less stiffen at about load level 1kN, and when the deformations of an element becomes outstanding, the element stiffens in terms of both axial deformation and mid-span deflection; obviously the mid-span deflection decreases significantly compared to the axial deformation. It means the resistance of an element against the transverse load relies on the axial stiffness due to large geometry change instead of bending action. It in turn heralds to release the reserve of strength of an element. Therefore, the present method is capable of capturing the large deformation behaviour, such as the catenary action. However, it is noteworthy to remark that the present method exploits 4 elements, whereas NIDA [16] and Iu and Bradford [3][4] use 4 and 8 elements, respectively. It is impossible to base on an element to reproduce the large deformation behaviour of a member no matter which numerical method or the finite element in the open literature is resorted to, because the axial component of an element cannot render to any transverse component without recourse to the transformation system, even though the terms $b_{m2}\overline{M}_0^2$ and $b_{s2}\overline{S}_0^2 L^2$ in Eq. 12 of the present method can contribute to the axial component solely due to transverse loads that are absent from other approaches. These axial components cannot be transformed into transverse components effectively by the element itself under this circumstance. It means the transverse load is impossibly taken by the axial resistance of an element, even when the deformations of an element become prominent. All axial components can only align along with the element, not in transverse direction, because the transformation of an element is merely formulated from two end nodes straightly. Hence, Figures 5 & 6 shows one present element can only simulate the linear elastic deflection and bending moment solutions, respectively.

Figures 5 & 6 illustrate the deflection and bending moment distribution along a simple supported beam at load level 9kN, which is also indicated at Figure 4 by the horizontal dashed line. In regard to the large deformation behaviour, 4 present higher-order elements are required to achieve the same accuracy of Iu and Bradford [3][4] when using 8 elements.

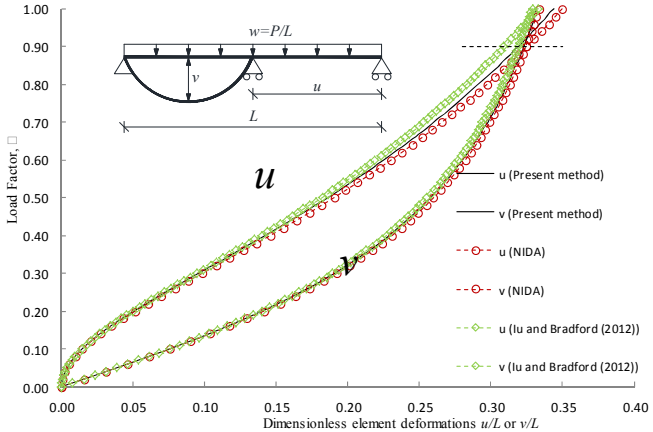

Figure 4. Large Deformation of a Simple Supported Element under Uniform Load

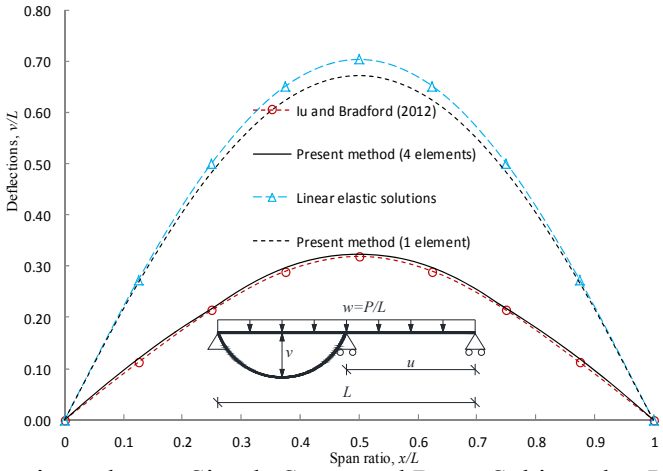

Figure 5. Deflections along a Simple Supported Beam Subjected to Large Deformation

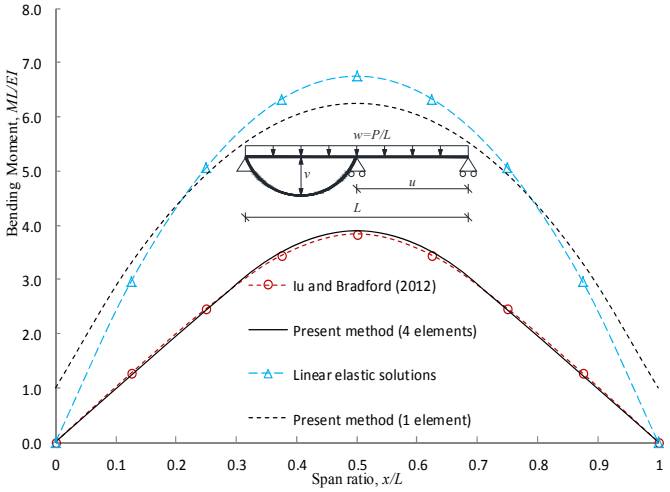

Figure 6. Bending Moment along a Simple Support Beam Subjected to Large Deformation

4.3 Second-order Sway Effect (P-Δ effect)

4.3.1 A cantilever subjected to uniform element load and axial compression

A cantilever is subjected to both transverse uniform distributed load, i.e. 10kN/m, and axial compression as given in Figure 7, and subsequently undergoes the P-Δ effect. On the basis of the numerical methods (including NIDA and present method), the load-deflection curves of the nodal axial u_L and transverse v_L deformations at tip are plotted in Figure 7, as well as the mid-span transverse deformation $v_{L/2}$ of the cantilever is given in Figure 7. It should be noted that the mid-span transverse deformation $v_{L/2}$ from NIDA (using 2 elements) is nodal solution, which is compared with the element solution from the present method. In Figure 7, the present method (1 element) is very consistent with the NIDA (1 element) in terms of all deformations. However, there is some discrepancy of the load-deflection curves from the present method (1 element) and NIDA (2 elements); especially the axial deformation after the buckling load at about 1.5 and at the post-buckling regime, when the cantilever exhibits axial stiffening due to catenary action. In general, all results from both approaches in terms of axial and transverse deformations are consistent.

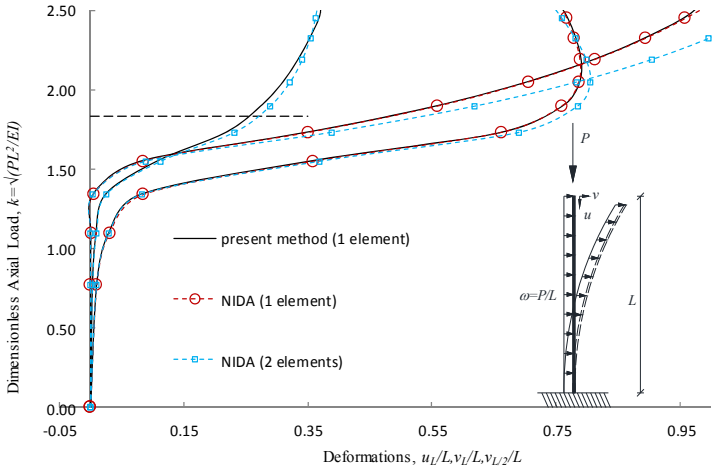

Figure 7. P-Δ Effect on a Cantilever with Uniform Distributed Load and Axial Compression

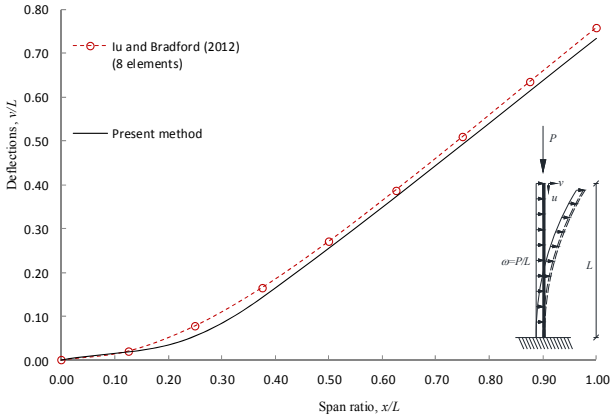

Figure 8. Deflections along a Cantilever Subjected to P-Δ Effect

In regard to the element displacement and force solutions, Figures 8 and 9 display the deflection and bending moment distribution along a cantilever at a specific level 1.83 (load factor λ=0.56), which is indicated by dash line in Figure 7. Similarly, the element responses, such as deflection and bending moment as respectively shown in Figures 8 & 9, from the present method are consistent with the nodal solutions from those of Iu and Bradford [3][4]. It is interesting to note that the rigid body motion is taken into account for P-Δ effect, whereas the bending moment is directly generated from the natural deformation of an element, such as its curvature. And the bending moment at the mid-span of an element is more accurate than other locations as noted and explained in [Iu [15]]. Further, it is remarked that this structure encounters the large deflection as well. Hence the example can also demonstrate that one proposed element is adequate to replicate the large deformation behaviour.

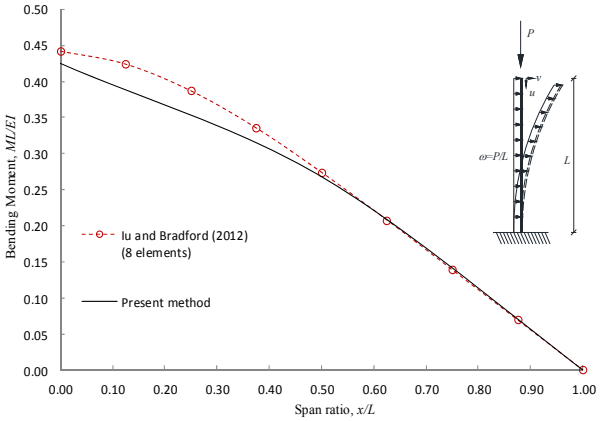

Figure 9. Bending Moment along a Cantilever Subjected to P-Δ Effect

4.3.2 A simple portal sway frame subjected to vertical uniform load only

A portal frame subjected to distributed uniform load ω=10kN/m is studied, of which the columns have an initial inclination of ψ=1/200 and the geometry and the properties are depicted in Figure 10. This example can verify the sway effect (P-Δ effect) of a portal frame. The lateral nodal displacement of the sway frame is normally of great concern for P-Δ effect, and hence the element solutions of the members are always ignored under this circumstance. Therefore, this example exemplifies the element displacements including the rigid body motions as well as the bending moment distribution of all members. The lateral nodal displacements u_L of the frame and element deflections $v_{L/2}$ at mid-span of the beam are plotted in Figure 10. In order to generate the accurate mid-span deflection of the beam, NIDA discretises the beam into 2 elements, whereas Iu and Bradford [3][4] makes use of 4 elements for each member, which implies the mid-span deflections are transformed into the nodal displacement from these approaches. Conversely, the present method relies on 1 element for each member to cater for both lateral nodal displacements u_L of a frame and vertical element mid-span deflection $v_{L/2}$ of the beam. Figure 10 shows all displacements are very consistent with each other. It is emphasized that the element solution (mid-span deflection $v_{L/2}$) from the present method can reach a good agreement with the nodal solution of both approaches from linear to second-order ranges before the numerical divergence at λ=2.8. It also remarks that the mid-span deflection $v_{L/2}$ of the beam is well predicted by the linear elastic solutions Δ_v in Figure 10 till λ=2.5; especially the mid-span deflection $v_{L/2}$ increases considerably at λ=2.6 because of the P-Δ effect.

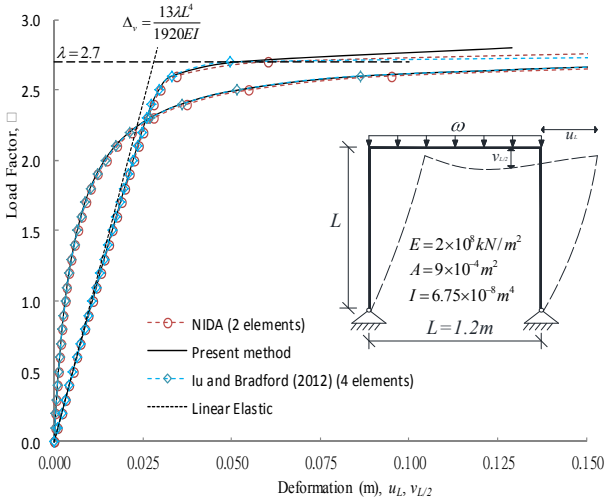

Figure 10. Mid-span Deformations of a Transversely Loaded Beam at the Sway Portal Frame

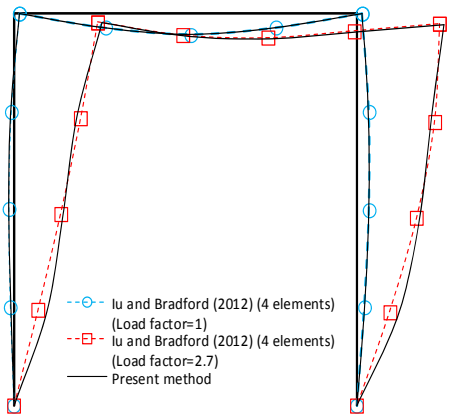

Figure 11. Deflection Shapes of the Sway Frame from Various Methods at λ=1 and λ=2.7

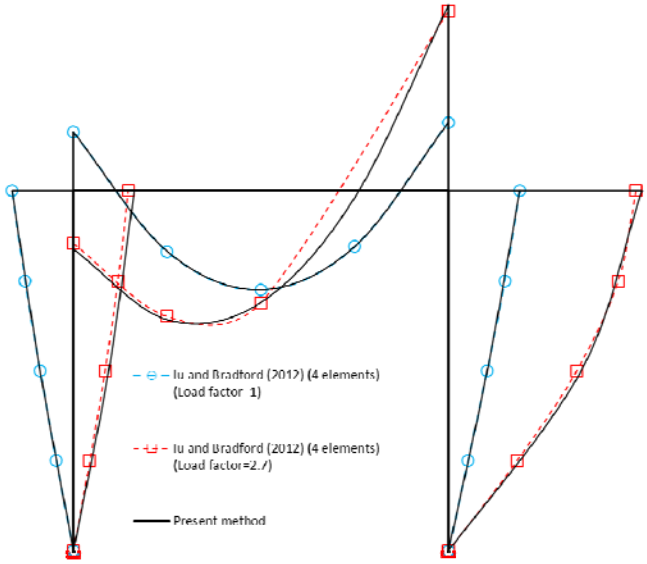

Figure 12. Bending Moments of the Sway Frame from Various Methods at λ=1 and λ=2.7

Figures 11 and 12 respectively illustrate the element solutions in terms of displacement and bending moment of all members of the sway frame at different load levels. In Figure 11, the element displacements (i.e. λ=1) from the present method are exactly same as the nodal displacements from the Iu and Bradford [3][4]. However, at λ=2.7, the deflections of the columns of the frame emerge slight discrepancy with the nodal solutions from Iu and Bradford [3][4] as given in Figure 11, which can be attributed to the solutions near the numerical instability at divergence. The accuracy of element solution is, however, still regarded to be reasonable. Similarly, the present method can generate the accurate bending moment along an element by itself, especially at its mid-span, when compared to those nodal solutions obtained from Iu and Bradford [3][4] as illustrated in Figure 12, but the discrepancy become obvious at load level λ=2.7.

4.4 Snap-through, Pre- and Post-buckling

4.4.1 A toggle frame subjected to the uniform distributed element load

A two-bar toggle frame, which originates from Williams [17] under a point load at its apex, was modified by Zhou and Chan [9][10] for the study of the snap-through buckling behaviour being influenced by uniformly distributed element load ω=1kN/m in global axis as given in Figure 13. Its

boundary condition, properties and geometry are depicted in Figure 13. This frame is used for validating the capacity of the present method to capture the snap-through, pre- and post-buckling responses of a member due to element load effect using one sophisticated higher-order element, in which the pre-buckling behaviour is regarded as the combination of P-δ and P-Δ effects; snap-through buckling is referred to the stiffness deterioration transit between pre- and post-buckling; post-buckling associates with the large deformation behaviour.

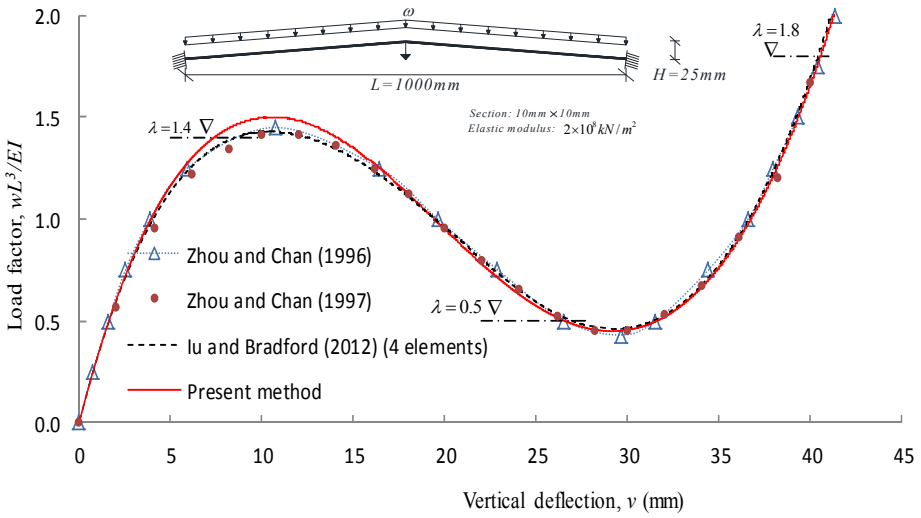

Figure 13. Load-deflection Curve at Top of Toggle Frame

The deflection at the top of toggle frame against the dimensionless load factor $\lambda=\omega L^3/EI$ is plotted in Figure 13 by using 4 elements for a member (Iu and Bradford [3][4]), which is well matched in all ranges by Zhou and Chan [9][10]. The present element load method using one element per a member cannot seamlessly replicate the accurate pre-buckling response of the toggle frame. The ultimate pre-buckling load is at λ=1.5 by virtue of the present method, whereas the pre-buckling load are at λ=1.43 and 1.45 from Iu and Bradford [3][4] and Zhou and Chan [9], respectively. Its accuracy is within the acceptable degree for engineering application. Apart from the pre-buckling regime, the snap-through and post-buckling behaviour of the toggle frame reach a good agreement with each other as shown in Figure 13. It is important to note that the disparity in pre-buckling behaviour may be attributed to the element load distribution being very sensitive to the pre-buckling behaviour, while the effect of element load distribution is converted into the single load magnitude of equivalent element load terms, such as $\overline{M}_0$ and $\overline{S}_0$, and therefore this effect is ignored in the higher-order element stiffness formulation.

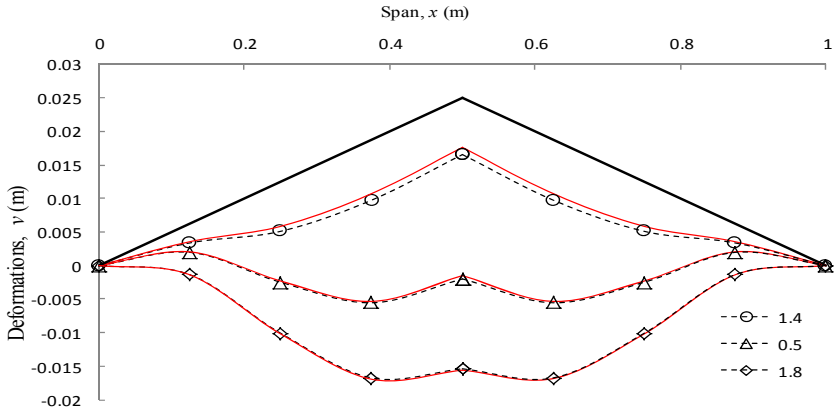

Figure 14. Deflection Shapes of Toggle Frame from Present Method and Iu and Bradford (2012)

at λ=1.4, λ=0.5 and λ=1.8

Figure 14 demonstrates that the present method using one element generates continuous element displacement solution of a member at different load factors as indicated by the solid lines, i.e. λ=1.4 (pre-buckling), λ=0.5 (snap-through buckling) & λ=1.8 (post-buckling), at which is also illustrated in Figure 13 by the dash-dot lines at respective levels. On the other hand, Iu and Bradford [3][4] produces the element deflections of a member by reliant on the nodal displacements as indicated by the dash lines with symbols in Figure 10. The accuracy of element deflection distributions among them is very consistent.

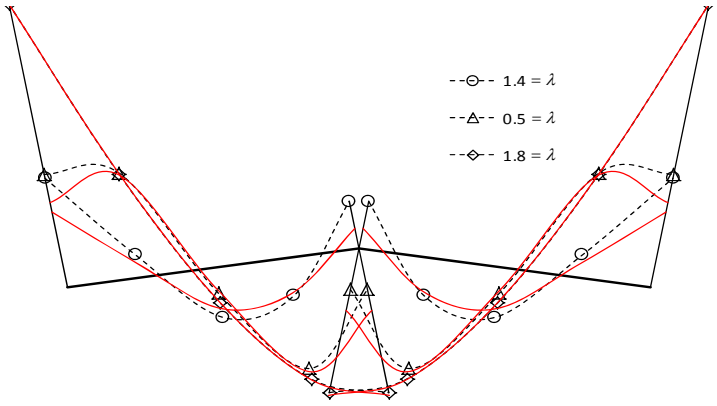

Figure 15. Bending Moments of Toggle Frame from Present Method and Iu and Bradford (2012) at λ=1.4, λ=0.5 and λ=1.8

Similarly, the element solutions in bending moment from the present method (solid lines) and Iu and Bradford [3][4] (dash lines with symbols) are given in Figure 15. The bending moment at the post-buckling level (λ=1.8) from the present method is very consistent with those from Iu and Bradford [3][4]. The distribution of bending moment at other load levels (λ=1.4 & 0.5) are also reasonably consistent between both methods.

4.5 Geometrical Initial Imperfection

4.5.1 Application of element load method for the imperfection of a member

According to Eurocode 3 [18], the assumed local imperfection of an element may be replaced by an equivalent transverse element load. In this sense, the present method can be extended to provoke the additional application to incorporate the initial imperfection along an element, which can degrade the stiffness of an element and trigger the member bowing effect prematurely. A dummy uniform distributed element load is imposed to include the local imperfection of an element, whose magnitude α_0 in turn represents the geometrical initial imperfection e_0. Hence, larger dummy load magnitude α_0 enables to cover larger allowance of geometrical imperfection e_0 of an element, of which the capacity of an element in deflection and internal moment resistance is deteriorated by the imperfection. For example, the buckling curves a_0, a, b, c and d in Eurocode 3 [18][17]. In principle, different α_0 can represent the corresponding buckling curves in the various design codes. A column having the equivalent initial imperfection α_0=0.01, 0.02 and 0.05 is under axial compression P=10kN, of which the mid-span deflection and bending moment are plotted in Figs. 16 and 17, respectively. They can be seen that the larger equivalent imperfection α_0 can stand for the larger buckling curves (i.e. c or d). Both Figures 16 & 17 demonstrate the deterioration of capacities when the equivalent imperfection becomes larger, but also approach to their elastic critical buckling load factor λ_E=0.164.

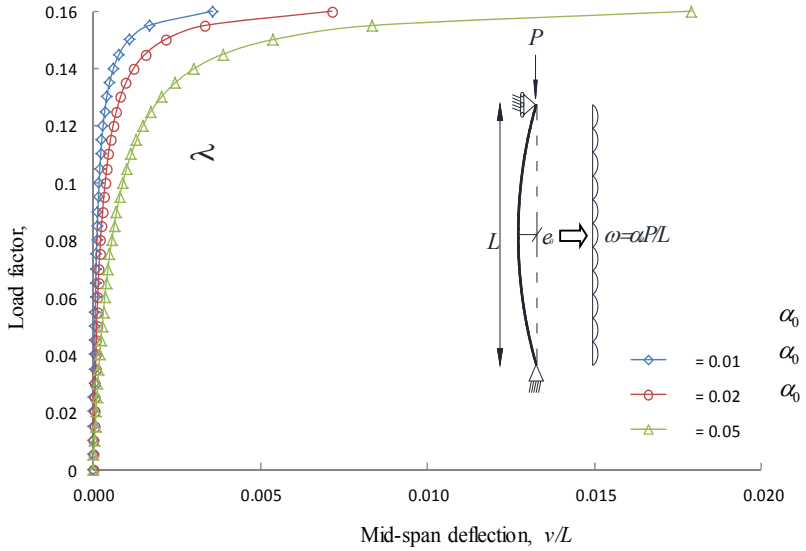

Figure 16. Deflection of a Column with Various Initial Imperfection α_0

It is noteworthy that, in numerical modelling viewpoint, if a perfect straight element is under axial compression, the flexural buckling behaviour can never be produced by that element because of no transverse component to trigger the second-order bowing effect. On the other hand, the incorporating equivalent imperfection α_0 through the GELM can allow for the modelling of flexural buckling using one-element-per-member approach. Hence no special consideration in the numerical modelling is required to capture second-order bowing effect, and thereby the present element facilitates the modelling preparation in the practical design.

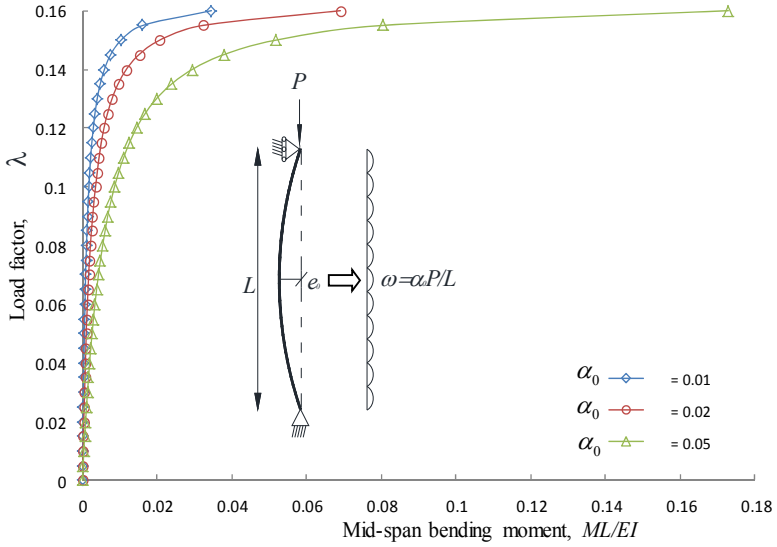

Figure 17. Bending Moment of a Column with Various initial imperfection α_0

5. DISCUSSIONS AND CONCLUSIONS

There are a few emphases from this paper as below;

- *Superposition principle valid in nonlinear solution procedure*
  The significant impact of this study is to impose the superposition principle as proved in this paper in order to generalise and unify the myriad of element load scenarios inherent in the standardised element stiffness formulation, e.g. Eqs. (8) to (12). In principle, this approach trades off the distribution of element load effect for the generality in element stiffness for a diverse kind of element load cases. In this sense, the distribution of element load is converted into a single magnitude of element load at mid-span of a sophisticated higher-order element. It leads to the same form of the element stiffness but various magnitudes of element load components (i.e. $\overline{M}_0 \& \overline{S}_0$) for various element load scenarios, which is succinctly customized from individual load case in the advent of nonlinear solution procedures. These element load components are then updated through the system solution procedures so that the second-order equilibrium path due to the coupling element load effect and the axial load can be traced successfully.
- *Inaccuracy in element load solution if sensitive to the element load distribution*
  This paper shows that the effect of the element load distribution is not sensitive to the typical buckling problem (i.e. P-δ effect) and thereby the application of superposition principle is valid. However, the slight discrepancy of the load-deflection relation is observed in the snap-through buckling behaviour, but still within the adequate level of accuracy in the engineering applications.
- *Superiority over other low- and higher-order element approaches*
  A) When the lower-order element function (e.g. cubic element or hierarchic h-version element) is exploited, the nonlinear equilibrium equation of a member must be linearized by dividing into a few low-order elements as known the element discretization. Moreover, the accuracy of the solutions by using the low-order element is inevitably restricted to the nodes. B) When the higher-order element, which is so-called one-element-per-member approach, is used to derive the higher-order element stiffness formulation that is adequate to solve the nonlinear equilibrium equation of a member by element itself. However, similarly the accurate element load solutions are resulted in at nodes only, because of no element load effects being incorporated into its stiffness formulation. C) On the other hand, the present approach extends the accurate solutions to both (discrete) nodal and (continuous) element solutions in both displacement and force fields. It heralds the element load solutions from the higher-order element formulation (generalised element load method - GELM) are commensurate with nodal solutions from the system analysis reasonably.

In summary, the present approach can possess robust capability of modelling the first- and second-order behaviour in terms of both nodal and element displacement and force solutions, which includes P-δ and P-Δ effect, large deformation behaviour, snap-through buckling, pre- and post-buckling and geometrical initial imperfection. In short, this paper can be therefore evolved into a unified method to yield accurate whole-domain (i.e. nodal and element) solutions of all kinds (i.e. displacement and force) under most regimes (i.e. first- and second-order elastic ranges), subjected to numerous element load scenarios. As a result, this GELM can ensure the reliable design (*thanks to whole-domain accuracy under most regimes*) of any civil engineering structure at the ultimate and serviceability limit states simultaneously (*thanks to both fields solutions*), especially indispensable to the one-element-per-member approach.

REFERENCES

[1] Meek, J.L. and Tan, H.S., "Geometrically Nonlinear Analysis of Space Frames by An Incremental Iterative Technique", Computer Methods in Applied Mechanics and Engineering, 1984, Vol. 47, pp. 261-281.

[2] Chan, S.L. and Kitipornchai, S., "Geometric Nonlinear Analysis of Asymmetric Thin-walled Beam-columns", Engineering Structures, 1987, Vol. 9, pp. 243-254.

[3] Iu, C.K. and Bradford, M.A., "Higher-order Non-linear Analysis of Steel Structures Part I: Elastic Second-order Formulation", Advanced Steel Construction, 2012a, Vol. 8, No. 2, pp. 168-182

[4] Iu, C.K. and Bradford, M.A., "Higher-order Non-linear Analysis of Steel Structures Part II: Refined Plastic Hinge Formulation", Advanced Steel Construction, 2012b, Vol. 8, No. 2, pp. 183-198.

[5] Chan, S.L. and Zhou, Z.H., "Pointwise Equilibrating Polynomial Element for Nonlinear Analysis of Frames", Journal of Structural Engineering, ASCE, 1994, Vol. 120, No. 6, pp. 1703-1717.

[6] Chan, S.L. and Zhou, Z.H., "Second-order Elastic Analysis of Frames Using Single Imperfect Element Per Member", Journal of Structural Engineering, ASCE, 1995, Vol. 121 No. 6, pp. 939-945.

[7] Izzuddin, B.A., "Quartic Formulation for Elastic Beam-columns Subject to Thermal Effects", Journal of Engineering Mechanics, ASCE, 1996, Vol. 122, No. 9, pp. 861-871.

[8] Iu, C.K. and Bradford, M.A., "Second-order Elastic Finite Element Analysis of Steel Structures Using a Single Element Per Member", Engineering Structures, 2010, Vol. 32, pp. 2606-2616.

[9] Zhou, Z.H. and Chan, S.L., "Refined Second-order Analysis of Frames with Members under Lateral and Axial Loads", Journal of Structural Engineering, ASCE, 1996, Vol. 122, No. 5, pp. 548-554.

[10] Zhou, Z.H. and Chan, S.L., "Second-order Analysis of Slender Steel Frames under Distributed Axial and Member Loads", Journal of Structural Engineering, ASCE, 1997, Vol. 123, No. 9, pp. 1187-1193.

[11] Neuenhofer, A. and Filippou, F.C., "Evaluation of Nonlinear Frame Finite-element Medels", Journal of Structural Engineering, 1997, ASCE, Vol. 123, No. 7, pp. 958-966.

[12] Neuenhofer, A. and Filippou, F.C., "Geometrically Nonlinear Flexibility-based Frame Finite Element", Journal of Structural Engineering, 1998, ASCE, Vol. 124, No. 6, pp. 704-711.

[13] Valipour, H.R. and Bradford, M.A., "Nonlinear P-Δ Analysis of Steel Frames with Semi-rigid Connections", Steel and Composite Structures, 2013, Vol. 14, No. 1, pp. 1-20.

[14] Iu, C.K. and Bradford, M.A., "Novel Non-linear Elastic Structural Analysis with Generalised Transverse Element Loads using Refined Finite element, Advanced Steel Construction, 2015, Vol. 11, No. 2, pp. 223-249.

[15] Iu, C.K., "Generalised Element Load Method for First- and Second-order Element Load Solutions", Engineering Structures, 2015, Vol. 92, pp. 101-111.

[16] Chan, S.L. and Zhou, Z.H., "On the Development of A Robust Element for Second-order "Nonlinear Integrated Design and Analysis" (NIDA), Journal of Constructional Steel Research, 1998, Vol. 47, pp. 169-190.

[17] Williams, F.W., "An Approach to the Non-linear Behaviour of Members of a Rigid Jointed Plane Framework with Finite Deflections, Quarterly Journal of Mechanics and Applied Mechanics, 1964, Vol. 17, No. 4, pp. 451-469.

[18] Eurocode 3: Design of Steel Structures – Part 1-1: General Rules and Rules for Buildings 2005.

APPENDIX I

The terms $G_{\alpha i}$ ($\alpha = y$ or z, $i = 1$ or 2) in Eq. 29 are:

$$\begin{aligned} G_{\alpha 1} = &\left\{\left[\frac{25600+4160q/7+92q^2/21+23q^3/1260}{(80+q)^3}\right](\theta_{\alpha 1}+\theta_{\alpha 2})\right. \\ &+\left[\frac{9216+1344q/5+132q^2/35+11q^3/420}{(48+q)^3}\right](\theta_{\alpha 1}-\theta_{\alpha 2}) \\ &\left.+\left[\frac{-16q}{35(48+q)^3}\overline{M}_0-\frac{16q}{63(80+q)^3}\overline{S}_0 L\right]\right\} \\ &=\frac{EI_\alpha}{L}\left\{2b_1(\theta_{\alpha 1}+\theta_{\alpha 2})+2b_2(\theta_{\alpha 1}-\theta_{\alpha 2})+b_{m1}\overline{M}_0+b_{s1}\overline{S}_0 L\right\} \end{aligned} \tag{30}$$

$$\begin{aligned} G_{\alpha 2} = &\left\{\left[\frac{25600+4160q/7+92q^2/21+23q^3/1260}{(80+q)^3}\right](\theta_{\alpha 1}+\theta_{\alpha 2})\right. \\ &-\left[\frac{9216+1344q/5+132q^2/35+11q^3/420}{(48+q)^3}\right](\theta_{\alpha 1}-\theta_{\alpha 2}) \\ &\left.+\left[\frac{16q}{35(48+q)^3}\overline{M}_0-\frac{16q}{63(80+q)^3}\overline{S}_0 L\right]\right\} \\ &=\frac{EI_\alpha}{L}\left\{2b_1(\theta_{\alpha 1}+\theta_{\alpha 2})-2b_2(\theta_{\alpha 1}-\theta_{\alpha 2})-b_{m1}\overline{M}_0+b_{s1}\overline{S}_0 L\right\} \end{aligned} \tag{31}$$

$$\begin{aligned} H = \frac{I}{AL^2} - \sum_{\alpha=y,z}\Big[&b_1'(\theta_{\alpha 1}+\theta_{\alpha 2})^2+b_2'(\theta_{\alpha 1}-\theta_{\alpha 2})^2+b_{m1}'(\theta_{\alpha 1}-\theta_{\alpha 2})\overline{M}_0 \\ &+b_{s1}'(\theta_{\alpha 1}+\theta_{\alpha 2})\overline{S}_0 L+b_{m2}'\overline{M}_0^2+b_{s2}'\overline{S}_0^2 L^2\Big] \end{aligned} \tag{32}$$

in which,

$$b_1' = -\left[\frac{102400/7+5120q/21}{(80+q)^4}\right]; \tag{33}$$

$$b_2' = -\left[\frac{36864/5+3072q/35}{(48+q)^4}\right]; \tag{34}$$

$$b_{m1}' = -\left[\frac{768-32q}{35(48+q)^4}\right]; \tag{35}$$

$$b_{m2}' = -\left[\frac{4/7+2q/105}{(48+q)^4}\right]; \tag{36}$$

$$b'_{s1} = -\left[\frac{1280 - 32q}{63(80+q)^4}\right]; \tag{37}$$

$$b'_{s2} = -\left[\frac{44/63 + 2q/315}{(80+q)^4}\right]. \tag{38}$$